

Numerical Modeling of Granular Salt

Brandon Lampe and Laxmi Paneru

May 6, 2015

Nomenclature

ϵ, ϕ = Volumetric and deviatoric strains
 σ_1, σ_3 = Maximum and minimum principal stresses
 Q_a = Activation energy
 R = Universal gas constant
 T = Absolute temperature
 t = Time
 C_1 = Constant factor

1 Introduction

Granular (or crushed) salt is a candidate material for sealing the Waste Isolation Pilot Plant's (WIPP) shafts, drifts, and boreholes [9]; therefore, the ability of crushed salt to prevent fluid migration is of interest. The objective of our research is to better understand the mechanical properties of crushed salt as they pertain to its transport properties. Most notably, we are interested in its intrinsic permeability, which will provide a direct measure of its adequacy as a sealing material. During recent laboratory tests, a correlation has been observed between the volumetric strain and the intrinsic permeability of crushed salt, where 20 percent volumetric strain has resulted in permeability decreasing by over nine orders of magnitude.

We have performed a laboratory test on crushed salt where the time dependent volumetric strain was measured while under a constant stress (creep). The objective of this paper is to determine if Abaqus contains a constitutive model capable of predicting the deformation observed during this experiment. Additionally, a comparison is made between results obtained using a general constitutive equation in Abaqus and results from a constitutive equation designed specifically for the modeling of crushed salt deformation.

The following sections will first familiarize the reader with the current state of crushed-salt constitutive models. Then a description of the laboratory experiment performed on a crushed-salt specimen is given. A brief description of the constitutive models

utilized to simulate the laboratory experiment are provided. Numerical results are then compared between constitutive models and our measured data in an attempt to determine if the selected models have the ability to capture characteristics shown in the laboratory experiment.

2 Literature Review

Mechanical properties of in situ salt were well characterized by Munson and Dawson during the early 1970's[8], where they first utilized an Arrhenius type equation to describe the time dependent deformation of salt (Equation 1), which is now common practice.

$$\dot{\epsilon}_{11} = C_1 * \exp\left(\frac{-Q_a t}{RT}\right) \quad (1)$$

During that same period, crushed salt became of interest to the engineering community also, predominately for use as a seal material around nuclear waste packages, shafts, and other openings associated with the storage of nuclear waste. The first recorded laboratory tests, performed for obtaining constitutive parameters, were uniaxial compression tests completed in 1978 on samples that were 5 centimeters in diameter [6]. However, the small specimen sizes utilized in these early tests resulted in nonuniform stress fields (from side and end friction) producing inconsistent results. Since the first tests on crushed salt were performed, testing techniques have advanced greatly and we are now able to accurately measures strains at at high temperatures and pressures that are representative of downhole conditions in a nuclear waste storage facility[2].

During the last 39 years, over ten constitutive models have been developed for crushed salt, each based on varying degrees of phenomenology, micro mechanics, and/or empiricism[4]. During the mid-1990's, the Crushed Salt (CS) Model was developed, which was the first model to combine several dominant deformation attributes of crushed salt. These attributes include grain boundary pressure solutioning and dislocation creep, which are believed to be

dominant deformation mechanisms of crushed salt [12, 13, 3]. Including these different deformation mechanisms is believed to be critical to accurately predicting the deformation of salt [5]. The CS Model has the ability to predict the deformation of crushed salt reasonably well at low temperatures, but at high temperatures Broome et al. [2] showed the model predictions did not well represent the true deformations. An additional shortcoming of the CS Model is the large number of material parameters (constants) associated with it, 31 independent parameters in total, which produce a highly nonlinear result that makes fitting parameters to a specific salt deposit very difficult. The US Dept. of Energy currently utilizes the CS Model to aid in there planning and development of storage facilities; therefore this model is of particular interest to us.

More recently, Olivella and Gens [10] developed an additional constitutive model that utilizes a nonlinear viscous approach that again focused on capturing the deformation associated with the active deformation mechanisms at different conditions. This model is currently employed by the THERESA project, which is a European based group aimed at developing, verifying and improving the modeling capabilities associated with the storage of nuclear waste. We do not currently have access to this model; therefore, this model will not be analyzed at this time.

3 Test Method

Experimental data was obtained during a hydrostatic creep test of a crushed salt specimen, approximate specimen geometry of the specimen was 200 mm in height and 100 mm in diameter (Figure 1). The test was performed over a 24-hour period (86,400 seconds) at a mean pressure of 20 MPa. Axial force was applied via a hydraulic ram and lateral force was applied via a low viscosity fluid that surrounded the vertical sides of the specimen. Axial displacements were measured with linear variable differential transformers (LVDTs) placed external to the specimen. Lateral deformations were measured with a pair of Schuler gages placed circumferentially around the specimen, and volumetric strains were measured directly with a dilatometer that metered the confining fluid volume in the test chamber.

Post test analyses revealed that deformations were approximately isotropic. Although, nonuniform deformation occurred near the ends of the specimen, where signs of end friction were observed. These signs included distinct cone shape regions near both ends of the specimen.

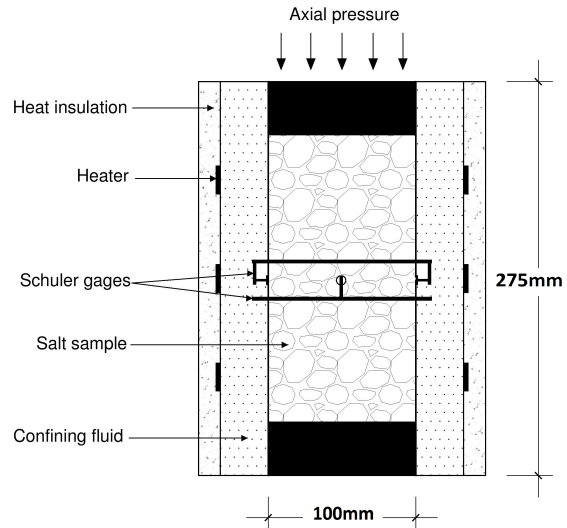


Figure 1: Representation of crushed-salt specimen in the triaxial cell.

4 Constitutive Models

Simulations of the time-dependent deformation during a creep tests were performed using the following constitutive models:

- linear isotropic viscoelasticity
- nonlinear isotropic viscoplasticity (CS Model)

The above models were chosen because they both predict time dependent deformation, which is an observed phenomena with crushed salt. The fundamental difference between two models are that one is elastic (no permanent deformation is predicted) and the other is plastic (allows for permanent deformation). Although a linear elastic constitutive model was not explicitly used, both of the above constitutive models assume that stress increments are the result of an elastic strain increment. Therefore, the following values were used in the formulation of the isotropic elasticity tensor:

- Young's Modulus: 5,625 MPa
- Poisson's Ratio: -0.75

The linear isotropic viscoelastic model was implemented in Abaqus [1]. However, Abaqus does not contain the CS Model in its constitutive library. Therefore, the constitutive equations for the CS Model were executed by a driver program written in the Python language. Abaqus utilized the finite

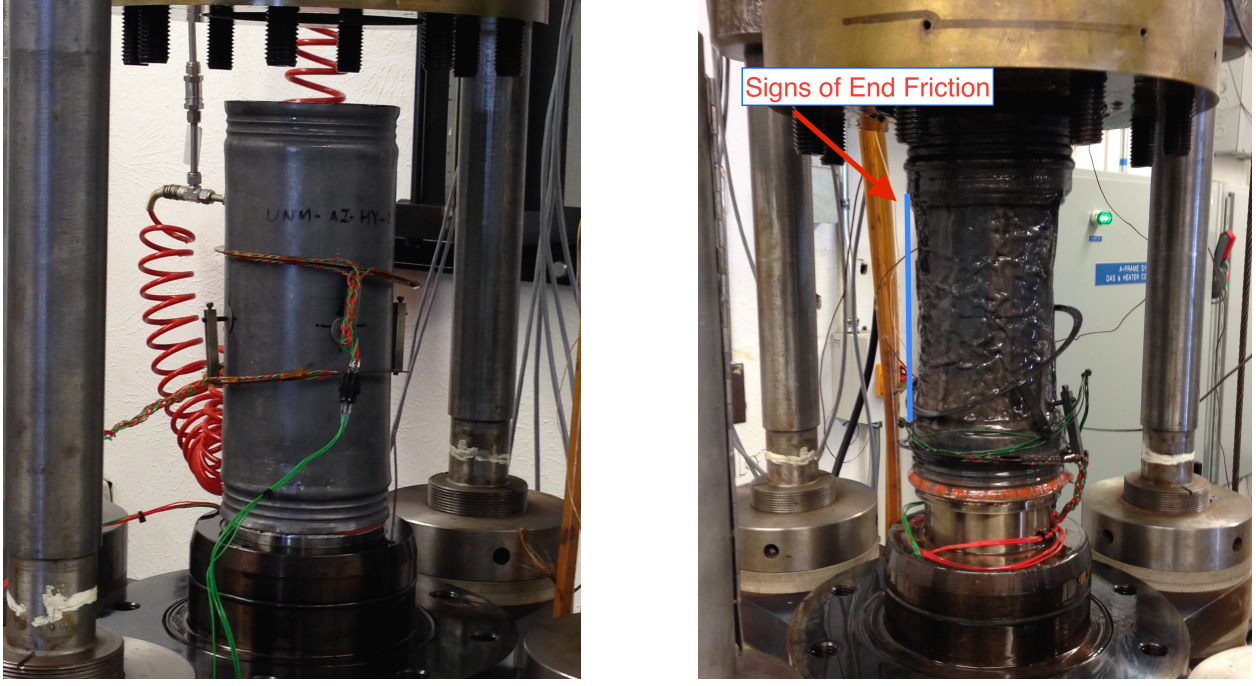


Figure 2: Pre (left) and post (right) test images of specimen in the test frame.

element method (FEM) to solve the complete set of field equations associated with the model (specimen and end platens), where the driver program merely solved the defined differential equations associated with the CS Model with the prescribed boundary conditions. Essentially, results from the driver program represent the solution for a single element discretization with boundary conditions applied directly to the specimen, whereas FEM allowed for boundary conditions to be applied upon adjacent materials where definitions of the interaction type were prescribed.

The linear viscoelastic model in Abaqus is a very general model that may be suited for modeling many different types of materials undergoing time dependent deformation. This generality is made possible by the user defining material specific parameters. Whereas the CS Model was specifically developed for the modeling of crushed salt. Because of its purpose-built nature, the CS Model contains many parameters not accounted for in the linear isotropic viscoelastic model, such as water content, grain size, and fractional density.

4.1 Linear Isotropic Viscoelasticity

The hereditary integral form for linear isotropic viscoelasticity under a prescribed stress was utilized by Abaqus (Equation 2). Stress was defined in terms

of a reduced (normalized) time (τ), which was related to the simulation time through Equation 3. The relaxation function and creep functions, ($K(\tau)$) and ($G(\tau)$), respectively, were also defined in terms of a normalized time using a series of exponentials known as a Prony series (Equations 4 and 5). Prony series parameters were fit using a least squares algorithm to creep test data in Abaqus CAE. The implemented linear visc constitutive equation utilized four material parameters (Equation 6). Because no shear data was made available for the Prony series calculations, the shear parameter G was defined as zero for all values of τ_i .

$$\sigma(t) = \int_0^t 2G(\tau - \tau')\dot{\epsilon}dt' + \mathbf{I}\int_0^t K(\tau - \tau')\dot{\phi}dt' \quad (2)$$

$$\tau = \int_0^t \frac{dt'}{A_\theta(\theta(t'))}, \quad \frac{d\tau}{dt} = \frac{1}{A_\theta(\theta(t))} \quad (3)$$

$$K(\tau) = K_\infty + \sum_{i=1}^2 K_i * \exp\left(\frac{-\tau}{\tau_i}\right) \quad (4)$$

$$G(\tau) = G_\infty + \sum_{i=1}^2 G_i * \exp\left(\frac{-\tau}{\tau_i}\right) \quad (5)$$

$$\begin{aligned} K(\tau_1) &= 0.685 & \tau_1 &= 2595.4 \\ K(\tau_2) &= -0.352 & \tau_2 &= 5.414 * 10^6 \end{aligned} \quad (6)$$

4.2 CS Constitutive Model

The CS Model contains mechanisms designed to capture the believed operative deformation mechanisms in crushed salt, namely dislocation creep and pressure solutioning. An assumption of the CS Model is that dislocation creep and pressure solutioning deformations are additive and the magnitudes of each depend on the current state of the crushed salt. The general form of the CS model provides a formulation of the plastic strain rate tensor ($\dot{\epsilon}^c$). Where the total predicted plastic strain is composed of both the inelastic strain rate measures for dislocation creep and pressure solution, $\dot{\epsilon}_{eq}^d$ and $\dot{\epsilon}_{eq}^w$, respectively. The magnitude of the respective strains are functions of an equivalent stress (σ_{eq}^f). Where The flow potential in the CS Model has been formulated in terms of an equivalent stress (σ_{eq}), which provides for a more flexible non-associative type flow.

The general form of the CS Model is provided in Equations 7 through 11, where $\eta_0, \eta_1, \kappa_0, \kappa_1, n_f, n$, and D_t are material parameters. Equation 12 describes the predicted strain resulting from pressure solutioning, where r_1, r_3, r_4, a, p , and Q are material parameters. Physical data, such as fractional density (D), water content (w), and grain size (d) are utilized as direct input into the constitutive model. Γ is a strain dependent variable, which is held at unity for small volumetric strain ($\exp(e_v) < 15\%$), which was the case for our simulations. The dislocation creep ($\dot{\epsilon}_{eq}^d$) equations are not listed here and the 20 parameters in that model were held constant at values suggested by Munson et al. [7]. The 13 parameters in the CS Model were fit using a Markov Chain Monte Carlo (MCMC) method, which was performed in the R programming language using the FME package [11].

$$\dot{\epsilon}^c = \left(\dot{\epsilon}_{eq}^d(\sigma_{eq}^f) + \dot{\epsilon}_{eq}^w(\sigma_{eq}^f) \right) \frac{\partial \sigma_{eq}}{\partial \sigma} \quad (7)$$

$$\sigma_{eq}^f = \left(\eta_0 \Omega_f^{\eta_1} \sigma_m + \left(\frac{2-D}{D} \right)^{\frac{2n_f}{n_f+1}} (\sigma_1 - \sigma_3)^2 \right)^{1/2} \quad (8)$$

$$\sigma_{eq} = \left(\kappa_0 \Omega_f^{\kappa_1} \sigma_m + \left(\frac{2-D}{D} \right)^{\frac{2n_f}{n_f+1}} (\sigma_1 - \sigma_3)^2 \right)^{1/2} \quad (9)$$

$$\Omega_f = \left[\frac{(1-D)_{n_f}}{(1-(1-D)^{\frac{1}{n_f}})^{n_f}} \right]^{\frac{2}{n_f+1}} \quad (10)$$

$$\Omega = \left[\frac{(1-D_v)_n}{(1-(1-D_v)^{\frac{1}{n}})^n} \right]^{\frac{2}{n+1}} \quad (11)$$

$$\dot{\epsilon}_w = \frac{r_1 w^a}{d^p \exp(e_v)} \frac{\exp\left(\frac{Q_s}{RT}\right)}{T} \left[\frac{\exp(r_3 e_v)}{\left(\exp(e_v) - 1\right)^{r_4}} \right] \Gamma \sigma_{eq}^f \quad (12)$$

5 Finite Element Modeling

The software package Abaqus/CAE 6.14-1 was utilized to perform finite element analyses using the linearly isotropic viscoelastic constitutive model. Multiple mesh discretizations of the salt specimen were created with a varying number of 8-node brick elements. Solutions for each of the discretizations were obtained and convergence of a solution was confirmed. Two planes of symmetry in the axial direction were utilized for the modeling, and because of this symmetry only a quarter of the model required discretization to obtain a solution to the three-dimensional problem (Figure 3). Simulations were performed with an array of discretizations to ensure sufficient element density was used for convergence of the solution (Table 1).

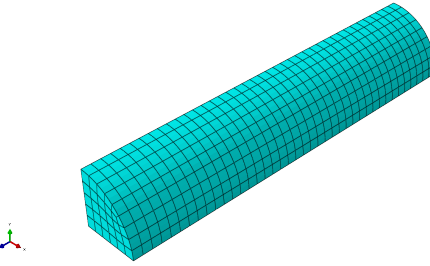


Figure 3: Finite element discretization of sample (h = 5 mm).

Element Length (h) [mm]	Elements	Nodes
100	6	62
50	12	108
20	30	246
5	1,160	6028

Table 1: Description of the discretizations used to simulate the crush-salt specimen.

Our model geometry consisted of two end platens modeled as linear elastic aluminum (Young's and

Poisson's moduli of 200 GPa and 0.3, respectively) and the test specimen, which was modeled as an linearly viscoelastic material. Both materials were assumed to be isotropic. Two orthogonal planes of symmetry were utilized for the model discretization, each having essential boundary conditions (zero displacement) applied normal to the plane of symmetry in radial directions (X and Y). The upper platen was also defined with an essential boundary condition of zero displacement in axial direction (Z). The lower platen and the curved face of the specimen were both defined as having essential boundary conditions (prescribed force). The boundary condition on the curved face of the specimen was defined as a constant pressure, which represents the normal stresses resulting from the confining fluid. Additionally, the lower platen was prescribed a constant normal pressure of 20 MPa in the Z direction.

Physical observations of the specimen indicated that sufficient end friction existed as to influence the deformation of the specimen (Figure 2). Therefore, interactions between the salt specimen and the end platens were also modeled in attempt to capture the influence of these affects.

6 Numerical Results

As part of the numerical analysis, a convergence study was completed to ensure that a sufficiently fine discretization had been employed. Data was obtained at a unique nodal point equidistant from the initial specimen ends along the Z axis, on the axis of symmetry. Very little deviation in results was shown across a large range of element sizes. The lack of deviation between mesh sizes ensures that a sufficiently refined mesh has been used. Additionally, if only average strains are desired, very few elements within the specimen are needed because of the modeled material and boundary conditions. That is, very few elements are needed because the problem is one of a hydrostatic stress being applied to an isotropic material. Results from this study are shown in Figure 5,

Displacement occurred in both the axial and radial directions during the the test (Figures 5). The influence of end friction was captured by the FE model, which is apparent by the additional stresses near the end of the specimen (Figure 6) and the reduced deformation near the specimen ends (Figure 7). When a more coarse mesh was utilized, the influence from the end platens was diminished.

Results from the CS Model and FE model both follow trends observed during the laboratory experi-

ment (Figure 8). Although, the CS Model over predicts the strain at early times, and the FE model under predicts these initial strains.

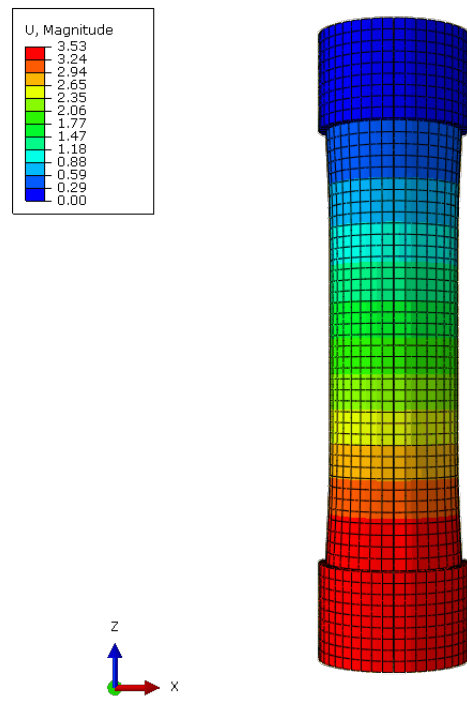


Figure 5: Magnitude of numerical displacements (mm) results from the isotropic linear viscoelastic simulation performed in Abaqus.

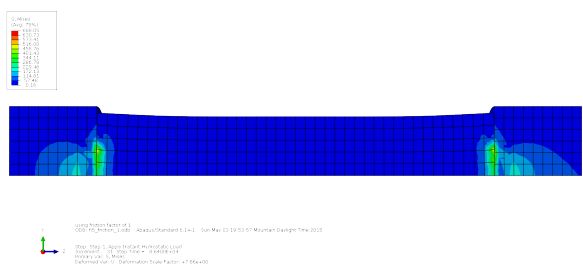


Figure 6: Mises resulting from friction between platens and specimen (dark blue indicates zero Mises stress).

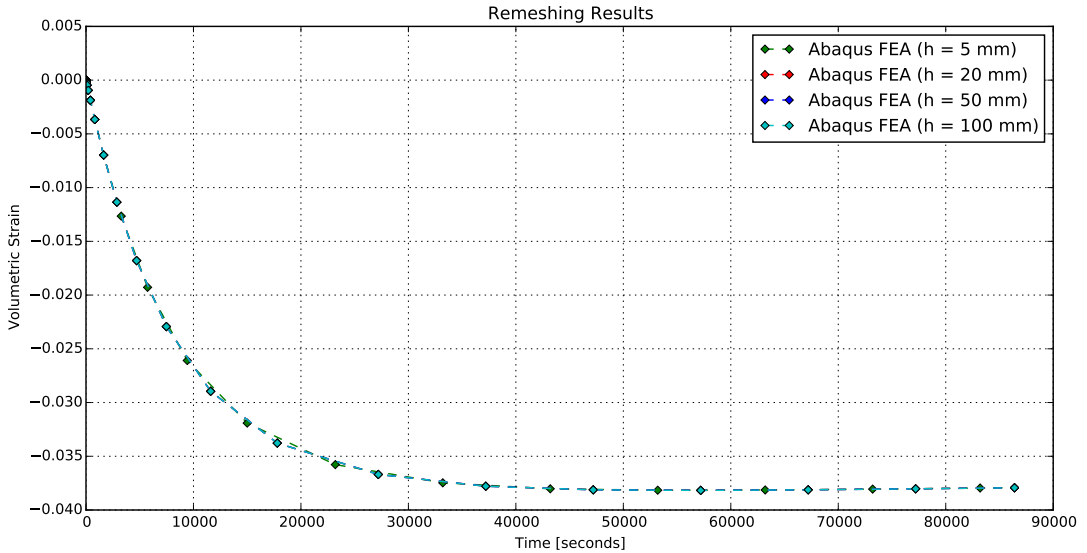


Figure 4: Numerical results from the convergence study.

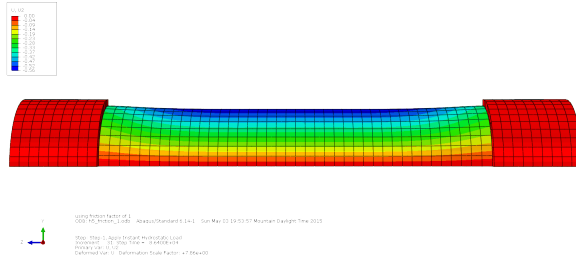


Figure 7: Cross-section of radial displacement, where red indicates zero.

7 Conclusions

Both constitutive models are capable of predicting volumetric strains similar to those measured during a creep test. The Abaqus model more closely represents the test data, but this is likely because Prony series values were fit exclusively to this loading path, whereas parameters of the CS Model were fit to a large range of loading paths.

Comparison of the predicted deformation at early times by the FE model to the experimental results that indicate that a model capable of predicting a higher level of early strains would be more suitable. This phenomena could likely be captured if a nonlinear viscoelastic model were utilized. Also, the over prediction of early strains by the CS Model may indicate that a nonlinear term could be removed from the model, or that the database used to fit material

parameters consisted largely of shear tests that often result in higher rates of initial strain.

The quality of both the CS Model and FE model to capture these specific test results are influenced greatly by the specific model parameters and how they were chosen. The CS Model parameters were fit to a large database that included both hydrostatic and shear tests, while the FE model was fit solely to the experimental data described herein. We believe the data used to fit the material parameters has a significant influence on the predicted results of both constitutive models.

To adequately validate the ability of the calculated Prony series utilized in the FE model, more loading paths must be simulated and compared to experimental data. Based on the present analysis, the linear viscoelastic constitutive model in Abaqus is capable of predicting the observed volumetric deformation of crushed salt during a creep test, but the correlation between experimental and simulated results may improve with the implementation of a nonlinear model.

References

- [1] Abaqus theory manual, 2012.
- [2] S.T. Broome, S.J. Bauer, and F.D. Hansen. Reconsolidation of crushed salt to 250 degrees celsius under hydrostatic and shear stress conditions. In *48th US Rock Mechanics / Geome-*

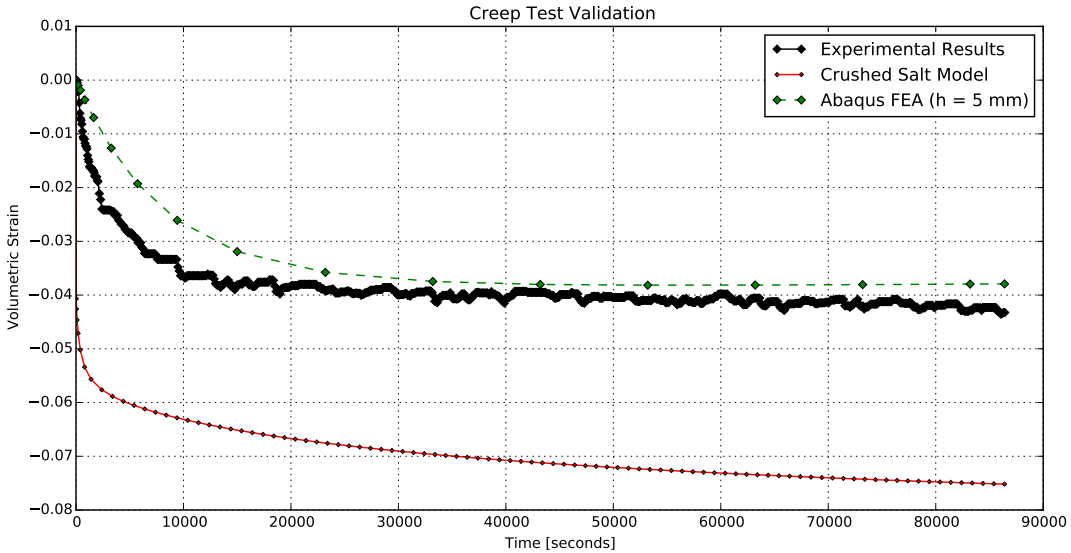


Figure 8: Comparison between experimental and predicted volumetric creep strain.

chanics Symposium held in Minneapolis, MN, USA, 1-4 June, 2014.

- [3] G. D. Callahan, K. D. Mellegard, and F. D. Hansen. Constitutive behavior of reconsolidating crushed salt. *International Journal of Rock Mechanics and Mining Sciences*, 35:422–423, 1998.
- [4] G.D. Callahan, M.C. Loken, L.L. Van Sambeek, R. Chen, T.W. Pfeifle, J.D. Nieland, and F.D. Hansen. Evaluation of potential crushed-salt constitutive models. Technical Report SAND95-2143, Sandia National Laboratories, 1995.
- [5] H.J. Frost and M.F. Ashby. *Deformation Mechanism Maps: The Plasticity and Creep of Metals and Ceramics*. Pergamon Press, 1982.
- [6] F.D. Hansen. Experimental consolidation of granulated rock salt with application to sleeve buckling. Technical Letter Memorandum RSI-0044, ReSpec, April 1976.
- [7] D. E. Munson, A. F. Fassum, and P. E. Senseny. Advances in resolution of discrepancies between predicted and measured in situ wipp room closures. Technical Report SAND88-2948, Sandia National Laboratories, 1989.
- [8] D.E. Munson and P. R. Dawson. Constitutive model for the low temperature creep of salt. Technical Report SAND79-1853, Sandia National Laboratories, 1979.
- [9] US Department of Energy. <http://www.wipp.energy.gov>. World Wide Web.
- [10] S. Olivella and A. Gens. A constitutive model for crushed salt. *International Journal For Numerical and Analytical Methods in Geomechanics*, (26):719–746, 2002.
- [11] Karline Soetaert and Thomas Petzoldt. A flexible modelling environment for inverse modelling, sensitivity, identifiability, monte carlo analysis. GPL >2, July 2014.
- [12] C.J. Spiers and R.H. Brzesowsky. Densification behaviour of wet granular salt: Theory versus experiment. In H. Kakihana, H.R. Jr. Hardy, T. Hoshi, and K. Toyokura, editors, *Seventh Symposium on Salt, Kyoto, Japan, April 6-9, 1992*, pages 83–92. Elsevier, 1993.
- [13] D.H. Zeuch. Isostatic hot-pressing mechanism maps for pure and natural sodium chloride: Application to nuclear waste isolation in bedded and domal salt formations. *International Journal of Rock Mechanics and Mining Sciences and Geomechanics Abstracts*, 27(6):505–524, 1990. SAND88-2207J.